JOURNAL OF NEUROTRAUMA 31:758–772 (April 15, 2014)

DOI: 10.1089/neu.2013.3194

# PARP-1 Inhibition Attenuates Neuronal Loss, Microglia Activation and Neurological Deficits after Traumatic Brain Injury

Bogdan A. Stoica,[1] David J. Loane,[1] Zaorui Zhao,[1] Shruti V. Kabadi,[1] Marie Hanscom,[1] Kimberly R. Byrnes,[2] and Alan I. Faden[1]

## Abstract

Traumatic brain injury (TBI) causes neuronal cell death as well as microglial activation and related neurotoxicity that contribute to subsequent neurological dysfunction. Poly (ADP-ribose) polymerase (PARP-1) induces neuronal cell death through activation of caspase-independent mechanisms, including release of apoptosis inducing factor (AIF), and microglial activation. Administration of PJ34, a selective PARP-1 inhibitor, reduced cell death of primary cortical neurons exposed to N-Methyl-N'-Nitro-N-Nitrosoguanidine (MNNG), a potent inducer of AIF-dependent cell death. PJ34 also attenuated lipopolysaccharide and interferon-$\gamma$-induced activation of BV2 or primary microglia, limiting NF-$\kappa$B activity and iNOS expression as well as decreasing generation of reactive oxygen species and TNF$\alpha$. Systemic administration of PJ34 starting as late as 24 h after controlled cortical impact resulted in improved motor function recovery in mice with TBI. Stereological analysis demonstrated that PJ34 treatment reduced the lesion volume, attenuated neuronal cell loss in the cortex and thalamus, and reduced microglial activation in the TBI cortex. PJ34 treatment did not improve cognitive performance in a Morris water maze test or reduce neuronal cell loss in the hippocampus. Overall, our data indicate that PJ34 has a significant, albeit selective, neuroprotective effect after experimental TBI, and its therapeutic effect may be from multipotential actions on neuronal cell death and neuroinflammatory pathways.

**Key words:** controlled cortical impact; microglial activation; neuroprotection; PARP-1; PJ34

## Introduction

More than 1.7 million new cases of traumatic brain injury (TBI) occur in the United States annually,[1] causing 60% of all trauma-related deaths.[2] TBI causes tissue loss and neurological dysfunction through delayed biochemical cascades (secondary injury) triggered by the primary mechanical injury.[3] Secondary injury mechanisms include neuronal loss from caspase-dependent and caspase-independent apoptotic cell death.[3] TBI also initiates a neuroinflammatory response that involves activation of microglia and astrocytes followed by release of neurotoxic molecules and delayed neuronal cell death. Targeting the molecular mechanisms that regulate both apoptosis and neuroinflammation may result in more effective therapeutic strategies for TBI.[4,5]

Poly (ADP-ribose) polymerase-1 (PARP-1; EC 2.4.2.30) is the most abundant member of a large family of enzymes[6] that utilize nicotinamide adenine dinucleotide (NAD+) to form and attach ADP-ribose polymers (PAR) onto glutamic acid residues of proteins.[7] PARP-1 is located in the nucleus and is responsible for the majority of cellular PARP activity. It is activated by DNA strand breaks caused by genotoxic stressors such as oxygen radicals or alkylating agents[8] leading to poly(ADP-ribosyl)ation of various nuclear proteins including PARP-1 itself[9] PARP-1 facilitates DNA base excision repair after DNA damage by poly(ADP-ribosyl)ation of histones, topoisomerases, and DNA polymerases, recruiting them to DNA break sites and altering DNA structure to make it more accessible to the repair proteins, thus maintaining genomic integrity and stability.[8,10] PARP-1 also regulates other important physiological processes including transcriptional activation,[11] chromatin remodeling and relaxation,[12] mitosis,[13] and DNA maintenance.[9]

PARP-1 activation, however, can also contribute to tissue damage after central nervous system injury, including ischemia[14,15] and trauma.[16,17] The mechanisms responsible for TBI-induced activation of PARP-1 include single strand DNA breaks produced by reactive oxygen and nitrogen species such as the hydroxyl radical and peroxynitrite.[18] Traditionally, PARP-mediated neuronal cell

[1]Department of Anesthesiology, Center for Shock, Trauma and Anesthesiology Research (STAR), National Study Center for Trauma and EMS, University of Maryland, School of Medicine, Baltimore, Maryland.
[2]Uniformed Services University of the Health Sciences, Bethesda, Maryland.

death was thought to follow an indirect energy failure mode reflecting consumption of NAD+ followed by adenosine triphosphate (ATP) depletion that results in passive cell death (necrosis). More recent studies focused on active PARP-1–mediated cell death pathways such as parthanatos, a form of PAR-induced and caspase-independent apoptosis executed through apoptosis inducing factor (AIF) release.[19,20] PARP may also directly mediate mitochondrial dysfunction, impairing mitochondrial respiration and decreasing ATP production through poly-ADP-ribosylation and inactivation of electron transport chain complex IV (cytochrome oxidase; COX) and/or glyceraldehyde 3-phosphate dehydrogenase (GAPDH), a key glycolytic enzyme.[21]

The role of poly-ADP-ribosylation as a mediator of mitochondrial dysfunction is supported by observation that decreasing PAR levels in conditions of nitrosative stress preserves mitochondrial respiration. PARP-1-dependent nuclear factor-kappaB (NF-$\kappa$B) activation can also trigger pro-inflammatory gene expression and microglia activation with release of multiple neurotoxic molecules (nitric oxide [NO], reactive oxygen species [ROS] and tumor necrosis factor-$\alpha$ [TNF$\alpha$]).[6,21] Thus, as the extent of DNA breaks increase, PARP-1 may cease to be a beneficial and restorative factor, and its DNA repair roles are overshadowed by activities contributing to increased cell injury.[22]

We hypothesized that PARP-1 plays key roles in specific models of neuronal cell death and microglial activation *in vitro* and that PARP-1-dependent neuronal cell death and neuroinflammation are important contributors to neuronal loss and neurological deficits after experimental TBI *in vivo*. The purpose of the present studies was to demonstrate using controlled cortical impact (CCI), a well-established experimental TBI-model, that PJ34 (N-(6-oxo-5,6-dihydro-phenanthridin-2-yl)-N,N-dimethylacetamide), a potent water soluble PARP-1 inhibitor,[23] exerts significant neuroprotective effects with a clinically relevant therapeutic window of as long as 24 h.

## Methods

### *Microglial cell cultures and treatments*

The murine BV2 microglial cell line was cultured in DMEM (11995, Invitrogen, Eugene, OR) supplemented with 10% fetal bovine serum (SH30070.03, Hyclone, Logan, UT), 1% penicillin/streptomycin (SV30010, Hyclone) at 37°C with 5% $CO_2$. Primary cortical microglia were harvested from 2-day–old postnatal Sprague-Dawley rat pups as described previously.[24] The cortices were carefully dissected from the whole brain, the meninges removed, and cortical tissue was homogenized in L15 media (SH30525.01, Hyclone). Tissue homogenate was centrifuged at 4°C for 10 min at 1000 rpm, and resuspended in DMEM:F12 (11330, Invitrogen, Eugene, OR) supplemented with 10% fetal bovine serum and 1% penicillin/streptomycin. Mixed glial cultures were incubated at 37°C with 5% $CO_2$. After 7–10 days in culture, the mixed glial cultures were shaken at 37°C for 1 h at 100 rpm to detach and collect primary cortical microglia with greater than 96% purity. Microglia were seeded onto 96 well plates at a density of 90,000 cells/well.

To examine the effects of PARP-1 inhibition on microglial activation, BV2 and primary microglia were pre-treated with PJ34 (1, 10, or 20 $\mu$M) for 1 h followed by the addition of either lipopolysaccharide (LPS; 100 ng/mL) or interferon-$\gamma$ (IFN$\gamma$; 2 ng/mL) for 24 h. Each experiment included $n = 6$ samples for each treatment.

### *NO assay*

NO released from activated microglia was measured using a Griess Reagent kit (G7921, Invitrogen, Eugene, OR) according to the manufacturer's instructions. Relative absorbance was measured at 560 nm using the Synergy HT Multi-Mode Microplate Reader (Biotek, Winooski, VT). A standard curve was used to calculate the amount of nitrite release by activated microglia in each sample (expressed in $\mu$M).

### *Western blotting*

BV2 microglia were pre-treated with PJ34 (10 or 20 $\mu$M) for 1 h before stimulation with LPS (100 ng/mL) for 24 h. BV2 microglia were solubilized in RIPA buffer and analyzed by SDS-PAGE and transferred onto nitrocellulose membrane. The immunoblots were probed with an anti-inducible nitric oxide synthase (iNOS) (1:3000, Enzo Life Sciences International, Inc., Plymouth Meeting, PA). $\beta$-actin (1:20,000, Sigma-Aldrich) was used as an endogenous control. Immune complexes were detected with the appropriate HRP-conjugated secondary antibodies (Goat anti-Rabbit, Goat anti-Mouse; Kirkegaard & Perry Laboratories, Inc., Gaithersburg, MD), and visualized using SuperSignal West Dura Extended Duration Substrate (Thermo Scientific). Chemiluminescence was captured on a Kodak Image station 4000R station (Carestream Health, Rochester, NY), and protein bands were quantified by densitometric analysis using Carestream Molecular Imaging Software. The data presented reflect the intensity of the target protein normalized to protein levels of the endogenous control in each sample (expressed in arbitrary units).

### *TNF$\alpha$ assay*

TNF$\alpha$ release from activated microglia was measured using a TNF$\alpha$ enzyme-linked immunosorbent assay kit (#558535, BD Biosciences, San Jose, CA) according to the manufacturer's instructions. Relative absorbance was measured at 450 nm using the Synergy HT Multi-Mode Microplate Reader (Biotek, Winooski, VT). A standard curve was used to calculate the amount of TNF$\alpha$ release by activated microglia in each sample (expressed in ng/mL).

### *NF-$\kappa$B activity assay*

BV2 microglia were seeded at $3 \times 10^5$ cells per well in a 96 well plate and were transfected with NF-$\kappa$B-luciferase reporter plasmid (0.15$\mu$g pGL4.32[luc2P/NF-$\kappa$B/Hygro]; Promega, Madison, WI) using Lipofectamine2000 (Invitrogen, Carlsbad, CA) according to the manufacturer's instruction. After incubating with DNA-lipofectamine mixtures, the cells were pre-treated with PJ34 (20 $\mu$M) for 1 h followed by the addition of LPS (100 ng/mL) for 8 h. The cells were washed twice with phosphate buffered saline and lysed with a reporter lysis buffer (Promega). Cell extracts were centrifuged at 12,000 × g for 1 min at 4°C, and the supernatant was stored − 80°C for the luciferase assay. Twenty $\mu$L of cell extract was mixed with 100 $\mu$L of the luciferase assay substrate reagent (Promega) at room temperature, and the luciferase activity was measured using a microplate luminometer (Synergy HT, BioTek Instruments, Winooski, VA). All values were expressed as fold induction over control. Each experiment included $n = 6$ samples for each treatment.

### *Intracellular ROS assay*

Intracellular ROS levels were measured using a 2′,7′-dichlorodihydrofluorescein diacetate ($H_2$DCFDA) fluorescence assay. Briefly, drug treated BV2 microglia were incubated with 10 $\mu$M $H_2$DCFDA (Molecular Probes, Eugene, OR) for 45 min at 37°C in 5% $CO_2$. Fluorescence was measured using excitation and emission wavelengths of 490 nm and 535 nm, respectively. All values were expressed as percentage of control.

### *Neuronal cell cultures and treatments*

Rat primary cortical neuronal (RCN) cultures were derived from rat embryonic (E17) cortices. Cells were seeded onto poly-d-

lysine-coated 96-well or 100-mm petri dishes (cell density $1 \times 10^6$/$cm^2$) and maintained in serum-free conditions using the B27 supplement as described previously.[25] RCN were cultured and then treated on DIV 7. To examine the neuroprotective effects of the PARP-1 inhibitor, PJ34, RCN were pre-treated with PJ34 (20 mM), BOC (Boc-aspartyl-fluoromethylketone; 100 mM), or combined PJ34 + BOC followed by the addition of the cell death inducer, N-Methyl-N'-Nitro-N-Nitrosoguanidine (MNNG; 50 $\mu$M), for 24 h. Each experiment included $n = 6$ samples for each treatment.

### *Lactacte dehydrogenase (LDH) release assay*

LDH release was measured using the CytoTox96 Non-Radioactive Cytotoxicity Assay kit (Promega, Madison, WI) according to the manufacturer's instructions. Relative absorbance was read at 492 nm using the Synergy HT Multi-Mode Microplate Reader (Biotek, Winooski, VT). All values were expressed as percentage of control.

### *Calcein assay*

After the LDH assay, the remaining media were aspirated, and the cells were washed once with 100 $\mu$L Locke's Buffer (154 mM NaCl, 5.6 mM KCl, 3.6 mM $NaHCO_3$, 2.3 mM $CaCl_2$, 5.6 mM Glucose, 5 mM Hepes, 1.2 mM $MgCl_2$, pH 7.4). Than 100 $\mu$L Locke's Buffer containing 5 $\mu$M Calcein (ALX-610-026-M001, Enzo Life Sciences, Farmingdale, NY) was added to each well, and the plate was incubated at 37°C, 5% $CO_2$ for 30 min at assess RCN cell viability. Absorbance was measured at 485 nm (excitation) and 528 nm (emission) using the Synergy HT Multi-Mode Microplate Reader (Biotek, Winooski, VT). All values were expressed as percentage of control.

### *Caspase-3-like activity assay*

For the in-plate fluorometric caspase-3-like activity assay, media were removed from the plates, and 50 $\mu$L of caspase assay buffer (10 mM HEPES/KOH, pH 7.4, 2 mM EDTA, 0.1% CHAPS, 5 mM dithiothreitol, 1 mM AEBSF, 10 $\mu$g/ml pepstatin A, 20 $\mu$g/ml leupeptin, and 10 $\mu$g/ml aprotinin) containing 20 $\mu$M Ac-DEVD-AMC (#ALX-260-031, Enzo Life Sciences, Farmingdale, NY) was added to each well. The plate was inserted immediately into a CytoFluor 4000 fluorometer, and free AMC accumulation, resulting from cleavage of the aspartate–AMC bond, was monitored continuously in each well over 1 h using 360 nm excitation and 460 nm emission wavelengths. Emission from each well was plotted against time. Linear regression analysis of the initial velocity (slope) of each curve yielded caspase-3-like activity for each sample. All values were expressed as percentage of control.

### *CCI TBI*

All surgical procedures were performed in accordance with protocols approved by the University of Maryland School of Medicine Institutional Animal Care and Use Committee. Our custom-designed CCI injury device[26] consists of a microprocessor-controlled pneumatic impactor with a 3.5 mm diameter tip. Male C57Bl/6 mice (20–25 g; Taconic Farms Inc.) were anesthetized with isoflurane evaporated in a gas mixture containing 70% $N_2O$ and 30% $O_2$ and administered through a nose mask (induction at 4% and maintenance at 2%). Depth of anesthesia was assessed by monitoring respiration rate and pedal withdrawal reflexes. Mice were placed on a heated pad, and core body temperature was maintained at 37°C. The head was mounted in a stereotaxic frame, and the surgical site was clipped and cleaned with Nolvasan and ethanol scrubs.

A 10-mm midline incision was made over the skull, the skin and fascia were reflected, and a 4-mm craniotomy was made on the central aspect of the left parietal bone. The impounder tip of the injury device was then extended to its full stroke distance (44 mm), positioned to the surface of the exposed dura, and reset to impact the cortical surface. Moderate-level injury was induced using an impactor velocity of 6 m/sec and deformation depth of 2 mm as described previously.[26] After injury, the incision was closed with interrupted 6-0 silk sutures, anesthesia was terminated, and the animal was placed into a heated cage to maintain normal core temperature for 45 min post-injury. All animals were monitored carefully for at least 4 h after surgery and then daily. Sham animals underwent the same procedure as injured mice except for the impact.

**3 h post-injury treatment study 1 (behavior).** The PARP-1 inhibitor, PJ34 (#ALX-270–289, Enzo Life Sciences, Farmingdale, NY), or vehicle (saline) was administered using a 3-day administration protocol (a total of 30 mg/kg/day) as described previously[23] with some modifications: A single systemic injection of PJ34 (30 mg/kg, intraperitoneally [IP]) was administered at 3 h post-injury followed by six repeated injections of PJ34 (10 mg/kg, IP) every 8 h starting from 24 h post-injury; $n = 12$ per group. A separate group of mice received sham-injury and served as non-injured controls ($n = 5$).

**3 h post-injury treatment study 2 (immunocytochemistry).** The PARP-1 inhibitor, PJ34, or vehicle (saline) was administered as described above; $n = 6$ per group. A separate group of mice received sham-injury and served as non-injured controls ($n = 3$).

**24 h post-injury treatment study (behavior).** The PARP-1 inhibitor, PJ34, or vehicle (saline) was administered as follows: A single systemic injection of PJ34 (30 mg/kg, IP) was administered at 24 h post-injury followed by six repeated injections of PJ34 (10 mg/kg, IP) every 8 h starting from 48 h post-injury; $n = 10$ per group. A separate group of mice received sham-injury and served as non-injured controls ($n = 5$).

### *Motor function evaluation*

Chronic motor function recovery was evaluated using a beam walk task, a method that is particularly good at discriminating fine motor coordination differences between TBI and sham-injured animals.[27] Briefly, mice were trained for 3 days to cross a narrow wooden beam 6 mm wide and 120 mm in length, which was suspended 300 mm above a 60 mm thick foam rubber pad. The number of foot-faults for the right hind limb was recorded over 50 steps on each day of testing, and a basal level of competence at this task was established before sham-injury or TBI with an acceptance level of <10 faults per 50 steps. The beam walk test was performed at 0 (immediately before CCI), 1, 3, 7, 14, and 21 days after TBI.

### *Cognitive function evaluation*

Spatial learning and memory was assessed using the Morris water maze (MWM) as described previously.[27] The Morris water maze protocol included 2 phases: (1) Standard hidden platform training (acquisition) and (2) standard probe test. A circular tank (100 cm in diameter) was filled with water (23 ± 2°C) that was made opaque with white Crayola non-toxic paint. The maze was surrounded by various extra maze cues on the wall of the room. A transparent platform (10 cm in diameter) was submerged 0.5 cm below the surface of the opaque water. Starting on post-injury day (PID) 14, sham-injured and TBI mice were trained to find the hidden submerged platform located in the northeast quadrant of tank for 4 consecutive days (PID 14–17). Mice

underwent four trials per day starting from a randomly selected released point (east, south, west, and north). Each mouse was allowed a maximum of 90 sec to find the hidden submerged platform, and mice that failed to find the platform within this time were placed onto the platform and allowed to remain on the platform for 25 sec on the first day of training and for 10 sec on subsequent training days.

The swim path, latency to platform, time spent in each zone, and velocity were recorded by computer-based Any-Maze automated video tracking system (Stoelting Co, Wood Dale, IL). Reference memory was assessed by a probe trial on PID 18. The platform was removed, and mice were released from the southwest position, and the time spent in each quadrant was recorded out of a maximum of 60 sec.

### *Lesion volume assessment*

Mice were euthanized and transcardially perfused with saline and 10% buffered formalin phosphate solution (containing 4% paraformaldehyde; Fisher Scientific, Pittsburg, PA) on PID 21. Lesion volume was determined based on the Cavalieri method as described previously.[28] The lesion area was outlined using Stereoinvestigator software (MBF Biosciences, Williston, VT) to obtain the final volume measurements.

### *Assessment of neuronal cell loss in the hippocampal subregions, cortex, and thalamus*

Stereoinvestigator software (MBF Biosciences) was used to count the total number of surviving neurons in the cortex, thalamus, as well as Cornu Ammonis (CA) 1, CA2/3, and dentate gyrus (DG) subregions of the hippocampus using the optical fractionator method of stereology, as described previously.[28]

### *Assessment of microglial morphology in the cortex*

Stereoinvestigator software (MBF Biosciences) was used to count the number of cortical microglia in each of the three microglial morphological phenotypes (namely, ramified, hypertrophic, and bushy) using the optical fractionator method of stereology as described previously.[28,29]

### *Immunocytochemistry*

Frozen coronal brain sections (20 $\mu$m) were stained with anti-MAP2 (#M3696, Sigma-Aldrich, St-Louis, MO) or anti-AIF (#sc-13116, Santa Cruz Biotechnology, Santa Cruz, CA) using standard immunocytochemistry techniques. The sections were incubated with Alexa Fluor 546 Goat anti-mouse (#INV-A11030, Life Technologies, Grand Island, NY) for 3 h, and TO-PRO-3 (#T3605, Life Technologies) was used as a counter stain. Imaging was performed using a Leica TCS SP5 II Tunable Spectral Confocal microscope (Leica Microsystems Inc., Bannockburn, IL).

### *Statistical analysis*

For the beam walk and acquisition trials of the MWM test, repeated measures one-way analysis of variance (ANOVA) was performed, followed by multiple pairwise comparisons using the Student Newman-Keuls *post-hoc* test. One-way ANOVA followed by multiple pairwise comparisons using the Student Newman-Keuls *post-hoc* test was performed for the other behavioral tests, neuronal cell counts, and microglial activation. One-tailed unpaired Student *t* test was used for the lesion volume. Statistical analysis was performed using SigmaPlot Program, Version 12 (Systat Software, San Jose, CA) or GraphPad Prism software, version 4.00 for Windows (GraphPad Software, Inc., San Diego, CA). Data were expressed as mean ± standard errors of the mean (SEM), and significance was determined at $p \leq 0.05$.

## Results

### *Microglial activation* in vitro *is attenuated by the PARP-1 inhibitor, PJ34*

To investigate the effect of PARP-1 inhibition in microglia, we used two well-established models of microglial activation in BV2 and primary microglia. In the first model, BV2 microglia were treated with LPS (100 ng/mL) with or without pre-treatment with a selective PARP-1 inhibitor, PJ34 (1, 10, or 20 mM). After 24 h, we analyzed a number of markers of microglial activation (NO release, iNOS expression, TNF$\alpha$ release, NF-$\kappa$B activity, and ROS generation). LPS stimulation significantly induced all studied markers of activation when compared with untreated controls ($p < 0.01$ or $p < 0.001$ for each, one-way ANOVA). PARP-1 inhibition by PJ34 pre-treatment significantly attenuated LPS-induced NO release starting at 10 $\mu$M PJ34 (Fig. 1A; $p < 0.001$), and LPS-induced iNOS expression was significantly reduced at 20 mM PJ34 (Fig. 1B; $p < 0.01$).

PJ34 treatment alone (20 $\mu$M) had no effect on iNOS expression. In addition, PJ34 pre-treatment significantly attenuated LPS-induced TNF$\alpha$ release starting at 10 mM PJ34 (Fig. 1C; $p < 0.001$), and LPS-induced NF-$\kappa$B activity was significantly attenuated by 20 mM PJ34 (Fig. 1D; $p < 0.01$). PJ34 treatment alone (20 $\mu$M) had no effect on NF-$\kappa$B activity. Furthermore, LPS-induced ROS generation in BV2 microglia was significantly attenuated at 20 $\mu$M PJ34 (Fig. 1E; $p < 0.01$). Similar results were obtained in primary cortical microglia where PARP-1 inhibition significantly attenuated LPS-induced NO release starting at 10 $\mu$M PJ34 (Fig. 1F; $p < 0.001$), and PJ34 pre-treatment significantly attenuated LPS-induced TNF$\alpha$ release at 20 mM PJ34 (Fig. 1G; $p < 0.001$).

We then used the pro-inflammatory cytokine, IFN$\gamma$, in a second model of microglial activation. BV2 microglia were treated with IFN$\gamma$ (2 ng/mL) with or without pre-treatment with PJ34 (1, 10, and 20 mM), and 24 h later we assessed microglial activation by measuring NO and TNF$\alpha$ release and ROS generation. IFN$\gamma$ stimulation significantly induced all markers of activation when compared with untreated controls ($p < 0.01$ or $p < 0.001$ for each, one-way ANOVA). PARP-1 inhibition by PJ34 pre-treatment significantly attenuated IFN$\gamma$-induced NO release at 20 $\mu$M PJ34 (Fig. 2A), and significantly attenuated IFN$\gamma$-induced TNF$\alpha$ release starting at 10 $\mu$M PJ34 (Fig. 2B). In addition, PARP-1 inhibition significantly attenuated IFN$\gamma$-induced ROS generation starting at 1$\mu$M PJ34 (Fig. 2C).

### *MNNG-induced neuronal cell death is attenuated by the PARP-1 inhibitor, PJ34*

MNNG is a well-known inducer of PARP-1 activation and neuronal cell death.[30] To compare the role of PARP-1 versus caspase activation as causal factors in MNNG-induced neuronal cell death, primary cortical neurons were treated with MNNG (50 mM) with or without pre-treatment with PJ34 (20mM), BOC (100 mM, a pan-caspase inhibitor), or combined PJ34 + BOC. After 24 h, we analyzed various well-established assays for cell death (LDH release, calcein fluorescence and caspase-3 activity). MNNG treatment significantly induced cell death when compared with untreated samples in the calcein and LDH release assays ($p < 0.001$ for each). Notably, the MNNG-induced decrease in calcein fluorescence (an indicator of cell viability) was significantly attenuated by pre-treatment with PJ34 ($p < 0.001$), but not by pre-treatment with BOC (Fig. 3A). Combined treatment with PJ34 + BOC enhanced cell viability over and above PJ34 treatment alone levels

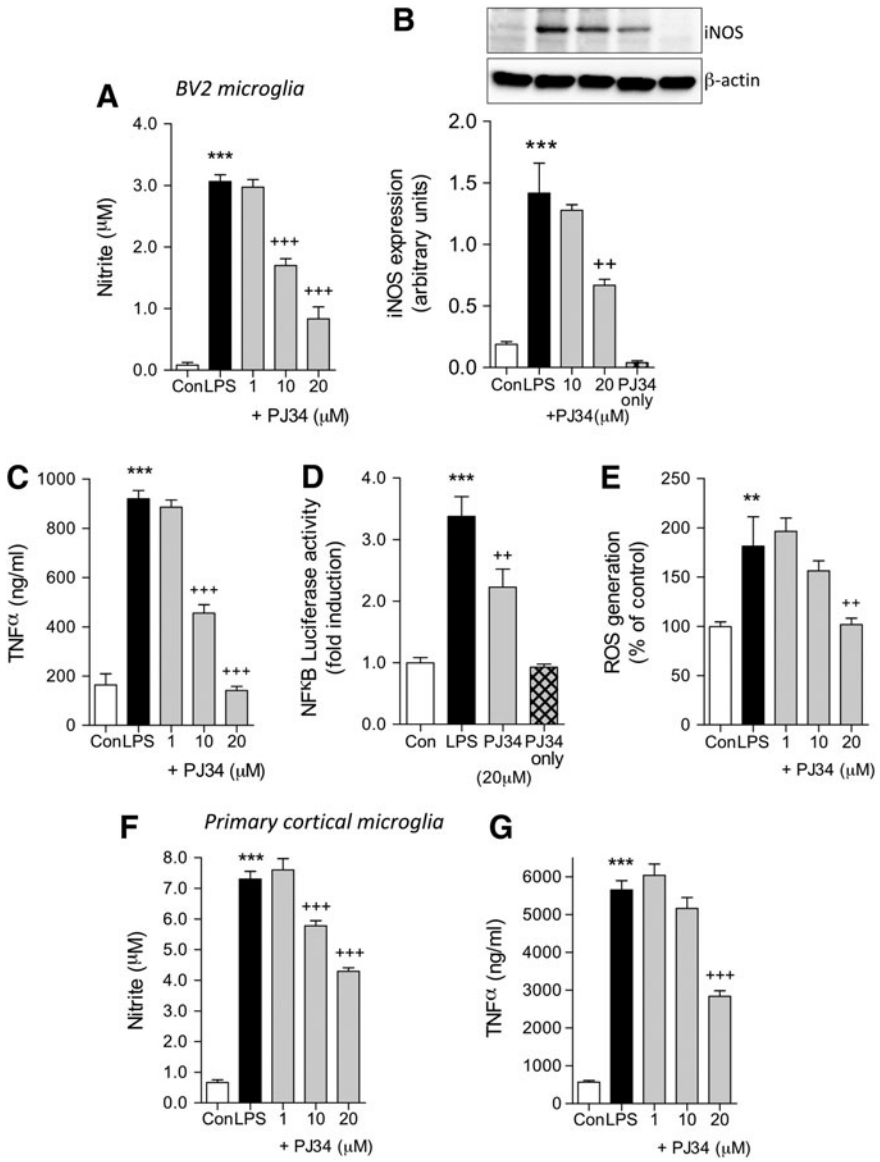


**FIG. 1.** PJ34 (N-(6-oxo-5,6-dihydro-phenanthridin-2-yl)-N,N-dimethylacetamide) attenuates lipopolysaccharide (LPS)-induced activation of BV2 microglia cell line and primary microglia. (**A**) LPS stimulation (100 ng/ml) in BV2 microglia significantly increased nitric oxide (NO) production (***$p<0.001$, LPS vs. control). PJ34 pre-treatment at concentrations of 10 $\mu$M and 20 $\mu$M attenuated LPS-induced NO production ($^{+++}p<0.001$, +PJ34 vs. LPS). (**B**) LPS stimulation in BV2 microglia significantly increased inducible nitric oxide synthase (iNOS) expression (***$p<0.001$, LPS vs. control). PJ34 pre-treatment (20 $\mu$M) attenuated LPS-induced iNOS expression ($^{++}p<0.01$, +PJ34 vs. LPS). Treatment with PJ34 alone had no effect on iNOS expression. (**C**) LPS stimulation (100 ng/mL) in BV2 microglia significantly increased TNFα production (***$p<0.001$, LPS vs. control). PJ34 pre-treatment at concentrations of 10 $\mu$M and 20 $\mu$M attenuated LPS-induced TNFα production ($^{+++}p<0.001$, +PJ34 vs. LPS). (**D**) LPS stimulation in BV2 microglia significantly increased nuclear factor-kappaB (NFκB) activity (***$p<0.001$, LPS vs. control). PJ34 pre-treatment (20 $\mu$M) attenuated LPS-induced NF-κB activation ($^{+++}p<0.001$, +PJ34 vs. LPS). Treatment with PJ34 alone had no effect on NF-κB activation. (**E**) LPS stimulation in BV2 microglia significantly increased reactive oxygen species (ROS) production (**$p<0.01$, LPS vs. control). PJ34 pre-treatment (20$\mu$M) attenuated LPS-induced ROS production ($^{++}p<0.01$, +PJ34 vs. LPS). (**F**) LPS stimulation in primary microglia significantly increased NO production (***$p<0.001$, LPS vs. control). PJ34 pre-treatment at concentrations of 10 $\mu$M and 20 $\mu$M attenuated LPS-induced NO production ($^{+++}$p$<0.001$, +PJ34 vs. LPS). (**G**) LPS stimulation in primary microglia significantly increased tumor necrosis factor α (TNFα) production (***$p<0.001$, LPS vs. control). PJ34 pre-treatment (20 $\mu$M) attenuated LPS-induced TNFα production ($^{+++}p<0.001$, +PJ34 vs. LPS). $n=6$ per treatment group. Mean ± standard error of the mean.

(Fig. 3A; $p<0.001$). MNNG treatment appeared to decrease caspase activity even below the levels in the control,suggesting it creates conditions not favorable for caspase activation in primary cortical neurons; intriguingly, pre-treatment with PJ34 (20 $\mu$M) resulted in a significant increase in caspase activation in response to MNNG treatment compared with both untreated and MNNG-treated samples (Fig. 3B; $p<0.001$). As expected pre-treatment with BOC, a powerful caspase inhibitor dramatically reduced caspase activity in both MNNG + BOC and MNNG + PJ34 + BOC samples (Fig. 3B). MNNG-induced LDH release (an indicator of

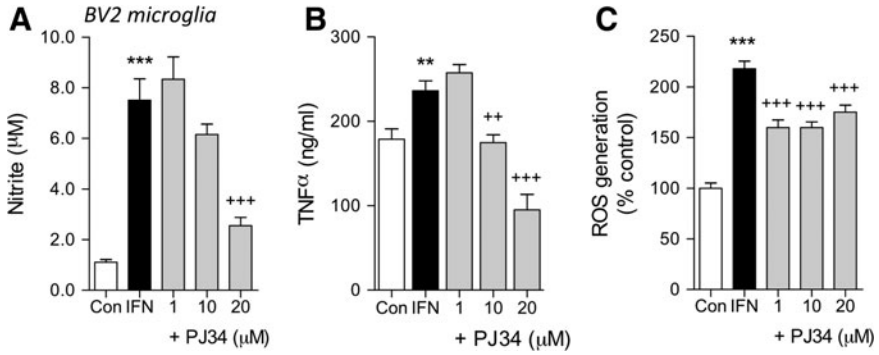


**FIG. 2.** PJ34 (N-(6-oxo-5,6-dihydro-phenanthridin-2-yl)-N,N-dimethylacetamide) attenuates interferon (IFN) $\gamma$-induced activation of BV2 microglia cell line. (**A**) IFN stimulation (2 ng/mL) significantly increased nitric oxide (NO) production (***$p < 0.001$, lipopolysaccharide [LPS] vs. control). PJ34 pre-treatment (20 $\mu$M) attenuated IFN-induced NO production ($^{+++}p < 0.001$, +PJ34 vs. IFN). (**B**) IFN stimulation significantly increased tumor necrosis factor $\alpha$ (TNF$\alpha$) production (**$p < 0.01$, LPS vs. control). PJ34 pre-treatment at concentrations of 10 $\mu$M and 20 $\mu$M attenuated IFN-induced TNF$\alpha$ production ($^{++}p < 0.01$, $^{+++}p < 0.001$, +PJ34 vs. IFN). (**C**) IFN stimulation significantly increased reactive oxygen species (ROS) production (***$p < 0.001$, IFN vs. control). PJ34 pre-treatment at concentrations of 1 $\mu$M, 10 $\mu$M, and 20 $\mu$M attenuated IFN-induced ROS production ($^{+++}p < 0.001$, +PJ34 vs. IFN). $n = 6$ per treatment group. Mean ± standard error of the mean.

cell death) compared with untreated samples (Fig. 3C; $p < 0.001$) was significantly attenuated by pre-treatment with PJ34 (Fig. 3C; $p < 0.001$). BOC pre-treatment alone had no effect on MNNG-induced LDH levels (Fig. 3C). Combined treatment with PJ34 + BOC did not significantly reduce the levels of LDH release over and above those for PJ34 treatment alone, although a trend was observed (Fig. 3C). Primary cortical neurons treated with PJ34, BOC, or PJ34 + BOC alone had the same levels as untreated controls in each of the outcome assays (data not shown).

### *The PARP-1 inhibitor, PJ34, improves motor function recovery and reduces lesion size but fails to reduce deficits in cognitive function when administered at 3 h post-injury*

Male adult C57Bl/6 mice underwent moderate level CCI and were treated with PJ34 (or vehicle) starting at 3 h post-injury. A single systemic injection of PJ34 (30 mg/kg, IP) was administered at 3 h post-injury followed by six repeated injections of PJ34 (10 mg/kg, IP) every 8 h starting from 24 h post-injury. A separate group of mice received sham-injury and served as non-injured controls.

To investigate the effect of PARP-1 inhibition on motor function recovery after TBI, mice were tested on the beam walk immediately before sham surgery or TBI and again on PID 1, 3, 7, 14, and 21. Repeated measures one-way ANOVA showed a statistically significant interaction between groups and time after injury ($F(8,125) = 6.541$, $p < 0.001$). TBI induced significant motor function impairments at all time points when compared with sham-injured mice (Fig. 4A; $p < 0.001$ for each PID). Notably, PJ34 treatment improved motor function recovery after TBI with a significant difference between the PJ34 TBI and vehicle TBI groups on PID 7, 14, and 21 ($p < 0.001$ for each PID).

To investigate the effect of PARP-1 inhibition on spatial learning and memory after TBI, we performed the MWM test from PID 14–17. Repeated measures one-way ANOVA showed a statistically significant interaction between groups and time after injury ($F(6,104) = 2.218$, $p = 0.047$). TBI induced significant cognitive function impairments at all time points in the vehicle TBI group when compared with the sham-injured group (Fig. 4B; $p < 0.05$ for PID 14, $p < 0.001$ for PID 15–17). PJ34 treatment in TBI mice, however, did not improve cognitive performance in this test, as indicated by the mean escape latency on PID 17 that was 78.40 ± 4.16 sec for PJ34 TBI and 83.43 ± 4.27 sec for vehicle TBI groups.

A probe trial was performed on PID 18. The hidden submerged platform was removed and the time sham and TBI mice spent in the target quadrant where the platform had originally been placed was recorded. Reduced time spent in the target quadrant indicated impaired reference memory. One-way ANOVA followed by Student Newman-Keuls *post-hoc* test indicated that both vehicle-treated and PJ34-treated TBI mice spent significantly less time in the target quadrant than sham-injured mice (Fig. 4C; $p < 0.05$ for both). No significant differences were observed between vehicle-treated and PJ34-treated TBI mice. Swim speeds did not differ between the sham-injured, vehicle-treated, and PJ34-treated TBI groups in this test (Fig. 4D).

TBI-induced lesion volume was quantified on cresyl violet-stained coronal brain sections from vehicle TBI and PJ34 TBI groups at PID 21 using stereological methods. TBI resulted in a large lesion in the vehicle-treated group (6.87 ± 0.46 $mm^3$) whereas PARP-1 inhibition significantly reduced the TBI-induced lesion volume in the PJ34-treated group (4.74 ± 0.90 $mm^3$) (Fig.5; $p = 0.025$, Student $t$ test). Representative images of vehicle TBI and PJ34 TBI groups are shown.

### *PARP-1 inhibition reduces TBI-induced neurodegeneration and the release of AIF from injured neurons*

A second cohort of C57Bl/6 mice underwent CCI and were treated with PJ34 at 3 h post-injury as described previously. All animals were euthanized at 72 h post-injury (after the last PJ34 dose), and brain sections were immunostained for markers of neurodegeneration and neuronal cell death. MAP2 is highly expressed in viable neurons and is lost from degenerating neurons. Our results revealed that in contrast to the robust MAP2 staining (red channel) that was observed across the cortex in the sham-injured group, samples from the vehicle-treated TBI group displayed a large contusion area with greatly reduced MAP2 immunostaining suggestive of degenerating neurons (Fig. 6A). In contrast, in the PJ34-

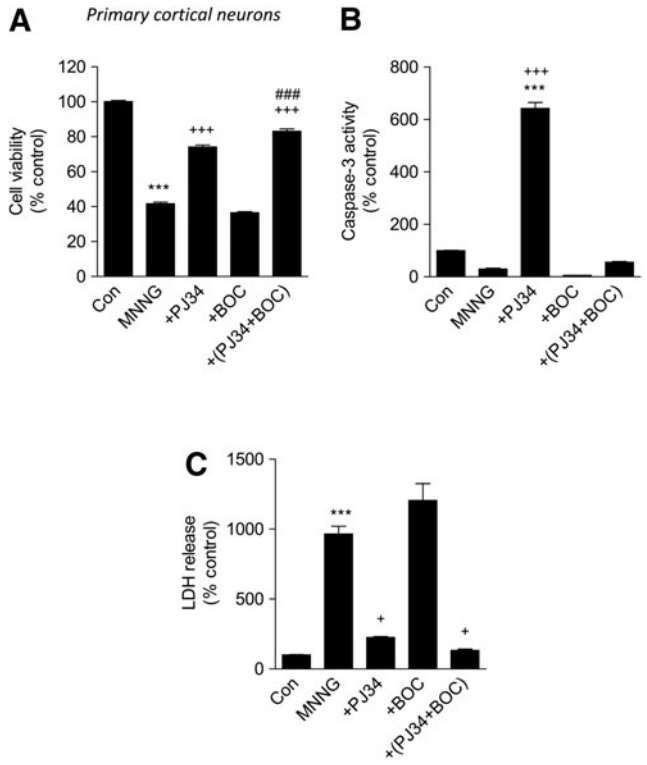


**FIG. 3.** PJ34 (N-(6-oxo-5,6-dihydro-phenanthridin-2-yl)-N,N-dimethylacetamide) attenuates N-Methyl-N'-Nitro-N-Nitrosoguanidine (MNNG)-induced neuronal cell death. (**A**) Calcein viability assay shows that MNNG (50 $\mu$M) treatment significantly reduces neuronal viability compared with control (***$p < 0.001$, MNNG vs. control). PJ34 (20 $\mu$M) pre-treatment (+PJ34) significantly attenuated MNNG-induced neuronal cell death ($^{+++}p < 0.001$, +PJ34 vs. MNNG). Pre treatment with the pan-caspase inhibitor Boc-aspartyl-fluoromethylketone (BOC) (100 $\mu$M) did not significantly attenuated MNNG-induced neuronal cell death. Pre-treatment with both PJ34 and BOC (+PJ+BOC) significantly attenuated MNNG-induced neuronal cell death ($^{+++}p < 0.001$, +PJ34+BOC vs. MNNG) and even improved on PJ34 neuroprotective effects ($^{###}p < 0.001$, +PJ+BOC vs. +PJ34). Analysis by one-way analysis of variance (ANOVA) (normality passed), followed by multiple pairwise comparisons using the Bonferroni *post-hoc* test. (**B**) Caspase activity assay shows that MNNG (50 $\mu$M) treatment does not increase caspase activity compared with control. PJ34 (20 $\mu$M) pre-treatment (+PJ34) significantly increases caspase activity compared with both control (***$p < 0.001$, +PJ34 vs. control) and MNNG-treated neurons ($^{+++}p < 0.001$, +PJ34 vs. MNNG). Pre-treatment with BOC (100 $\mu$M) alone or in conjunction with PJ34 (+PJ34+BOC) resulted in caspase activity levels at or below the levels in the control. Analysis by Kruskal-Wallis ANOVA based on ranks (normality failed), followed by multiple pairwise comparisons using the Dunn *post-hoc* test. (**C**) Lactate dehydrogenase (LDH) cell death assay shows that MNNG (50 $\mu$M) treatment significantly increases neuronal cell death compared with control (***$p < 0.001$, MNNG vs. control). PJ34 (20 $\mu$M) pre-treatment (+PJ34) significantly attenuated MNNG-induced neuronal cell death ($^{+}p < 0.05$, +PJ34 vs. MNNG). Pre-treatment with the pan-caspase inhibitor BOC (100 $\mu$M) did not significantly attenuate MNNG-induced neuronal cell death. Pre-treatment with both PJ34 and BOC (+PJ+BOC) significantly attenuated MNNG-induced neuronal cell death ($^{+}p < 0.05$, +PJ34+BOC vs. MNNG). Analysis by Kruskal-Wallis ANOVA based on ranks (normality failed), followed by multiple pairwise comparisons using Dunn *post-hoc* test. $n = 6$ per treatment group. Mean ± standard error of the mean.

treated TBI group, the area of the contused cortex with low MAP2 immunostaining was reduced (Fig. 6A). TO-PRO®-3 (DNA label marking the cell nuclei; blue channel) was used as a counterstain to indicate the presence of cells, and TO-PRO-3 staining was preserved in the contusion area indicating that low MAP2 staining was not because of the absence of cells but instead reflects neuronal degeneration.

AIF staining intensity is low in viable neurons when the protein is located in mitochondria, but is increased in neurons undergoing AIF-mediated cell death when AIF is released from mitochondria into the cytosol and translocates to the nucleus.[31,32] Slemmer and colleagues[31] have speculated that increased AIF staining intensity in the brain after TBI reflects better accessibility of the AIF protein to antibodies after release from mitochondria; this phenomenon was confirmed in previous studies from our group using the CCI model in mice.[32]

Our results indicate that in contrast to the low level AIF immunostaining (red channel) that was observed in the cortex in the sham-injured group, samples from the vehicle-treated TBI group displayed increased AIF immunostaining within the large contusion area, suggestive of AIF translocation from the mitochondria into the cytosol in damaged neurons after TBI (Fig. 6B). In contrast, the area and intensity of AIF immunostaining in the contused cortex of samples from the PJ34-treated TBI group animals was reduced.

TO-PRO-3 (blue channel) was used to counterstain nuclei of cells, and higher magnification images revealed that AIF had a punctate distribution outside of the nuclei in the sham-injured cortex, consistent with mitochondrial localization. Conversely, AIF immunostaining intensity was increased and widely distributed throughout the cell including the nucleus of neurons within the TBI cortex (superimposed with the TO-PRO-3 staining), suggestive of AIF release from the mitochondria into the cytosol with nuclear translocation (Fig. 6B). These changes were attenuated after administration of PJ34.

### *Delayed treatment with PJ34 improves motor function recovery and reduces lesion size when administered at 24 h post-injury*

Based on the robust improvements in motor function recovery after administration of PJ34 at 3 h post-injury, we investigated if we could expand the therapeutic window for PJ34 treatment and improve the clinical translation of PARP-1 inhibitors for TBI. Male adult C57Bl/6 mice underwent CCI and were treated with PJ34 (or vehicle) starting at 24 h post-injury. A single systemic injection of PJ34 (30 mg/kg, IP) was administered at 24 h post-injury followed by six repeated injections of PJ34 (10 mg/kg, IP) every 8 h starting from 48 h post-injury. A separate group of mice received sham-injury and served as non-injured controls.

To investigate the effect of delayed treatment of PJ34 on motor function recovery after TBI, mice were tested on the beam walk immediately before sham surgery or TBI and again on PID 1, 3, 7, 14, and 21. Repeated measures one-way ANOVA showed a statistically significant interaction between groups and time after injury ($F(8,110) = 6.029$, $p < 0.001$). Student Newman-Keuls *post-hoc* analysis revealed that TBI induced significant motor function impairments at all time points when compared with sham-injured mice (Fig. 7A; $p < 0.001$ for each PID). Notably, PJ34 treatment improved motor function recovery after TBI with a significant difference between the PJ34 TBI and vehicle TBI groups on PID 3 ($p < 0.01$), 7 ($p < 0.001$), 14 ($p < 0.001$), and 21 ($p < 0.001$).

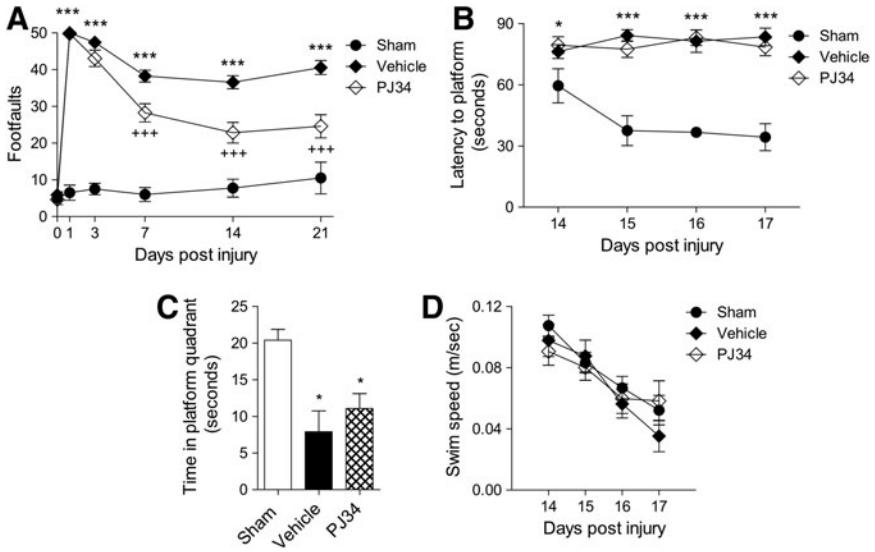


**FIG. 4.** Early systemic administration of PJ34 (N-(6-oxo-5,6-dihydro-phenanthridin-2-yl)-N,N-dimethylacetamide) improves sensorimotor function but not cognitive performance after traumatic brain injury (TBI). (**A**) Fine motor coordination deficits were quantified using the beam walk test. Hind-limb foot placement was recorded and the number of mistakes (foot faults) was recorded from 50 steps. TBI induced significant impairment in motor outcomes at all time points (***$p < 0.001$ vs. sham). There was a statistically significant ''post-injury day X groups'' interaction ($F(8,125) = 6.541$, $p < 0.001$). Systemic administration of PJ34 starting at 3 h post-injury significantly improved fine motor coordination at 7, 14, and 21 days ($^{+++}p < 0.001$ vs. vehicle) post-TBI. Analysis by repeated measures one-way analysis of variance (ANOVA), followed by multiple pair-wise comparisons using the Student Newman-Keuls *post-hoc test*. Mean ± standard error of the mean (SEM). $n = 12$ TBI groups, $n = 5$ sham-injured group. (**B**) Systemic administration of PJ34 starting at 3 h post-injury did not improve cognitive performance in the Morris water maze (MWM) test after TBI. Spatial learning and memory was assessed using the MWM test. The factors of ''post-injury days'' and ''groups'' were not statistically significant. TBI induced significant cognitive impairments at post-injury days 14, 15, 16, and 17 (*$p < 0.05$ vs. sham, ***$p < 0.001$ vs. sham). PJ34-treated TBI mice demonstrated a latency to locate the submerged platform that was not significantly different compared with vehicle-treated TBI mice. (**C**) In the probe trial, vehicle- and/or PJ34-treated TBI mice spent significantly less time in the target quadrant compared with sham-injured mice (*$p < 0.05$). No significant differences were observed between vehicle- and PJ34-treated TBI mice. (**D**) No significant differences in swim speed were observed between sham, vehicle-treated, and PJ34-treated TBI mice. Analysis by repeated measures one-way ANOVA (A, B, D) and one-way ANOVA (C), followed by multiple pairwise comparisons using the Student Newman-Keuls *post-hoc* test. Mean ± SEM ($n = 12$ TBI groups, $n = 5$ sham-injured groups).

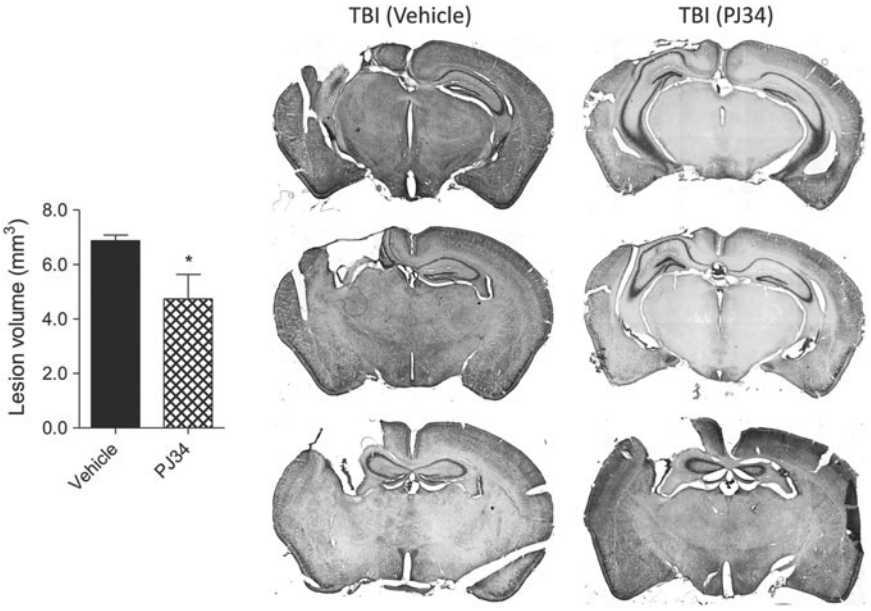


**FIG. 5.** Systemic administration of PJ34 (N-(6-oxo-5,6-dihydro-phenanthridin-2-yl)-N,N-dimethylacetamide) reduces lesion size after traumatic brain injury (TBI). Unbiased stereological assessment of lesion volume at 21 days post-TBI was performed on cresyl violet-stained brain sections. PJ34 treatment significantly reduced the lesion size at 21 days post-TBI (*$p < 0.05$ vs. vehicle). Analysis by one-tailed Student *t* test. Mean ± standard error of the mean ($n = 10$/group). Coronal sections across the TBI contusion/lesion from a representative animal in the vehicle-treated and PJ34-treated TBI groups are presented.

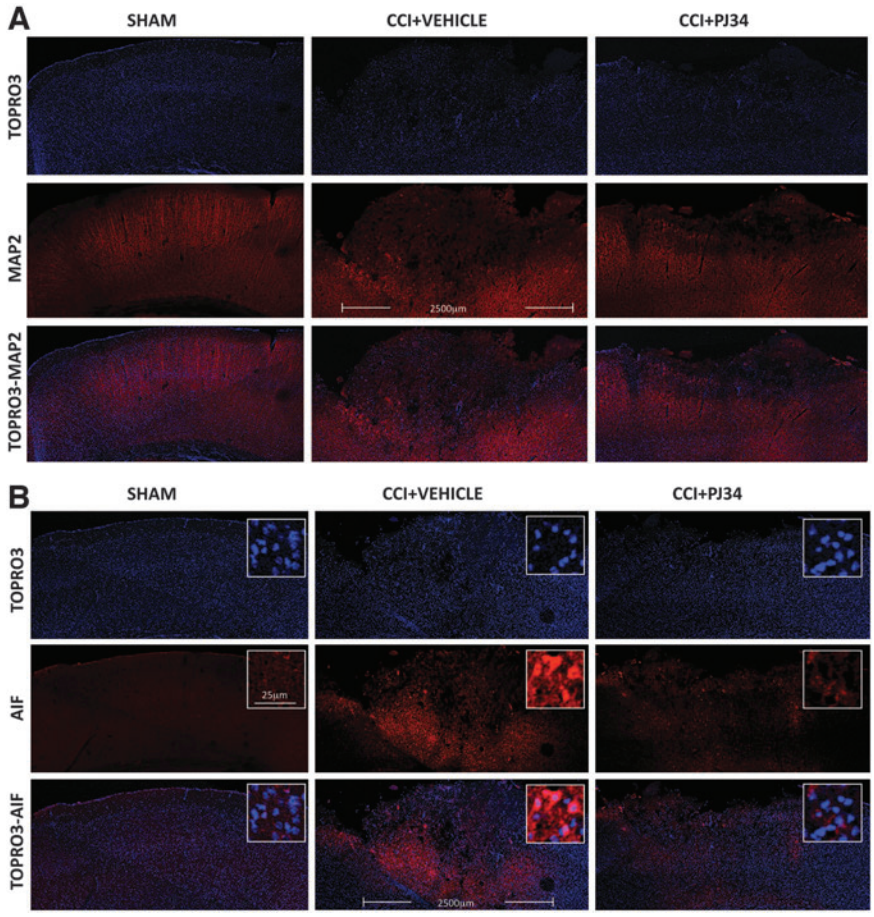


**FIG. 6.** Early systemic administration of PJ34 (N-(6-oxo-5,6-dihydro-phenanthridin-2-yl)-N,N-dimethylacetamide) attenuates neurodegeneration and apoptosis inducing factor (AIF) release after trsumatic brain injury (TBI). (**A**) Immunocytochemistry showed that vehicle-treated animals had decreased expression of MAP2 (a marker of neuronal viability; red channel) 72 h after trauma. TO-PRO-3 counterstaining (blue channel) demonstrates that cells are present in the contusion area. In comparison, animals that received systemic administration of PJ34 starting at 3 h post-TBI demonstrated increased MAP2 signal. (**B**) Immunocytochemistry also showed that vehicle-treated animals had increased in the AIF signal intensity 72 h after trauma reflecting the release of the pro-apoptotic protein AIF from mitochondria, a key step in the activation of AIF-mediated cell death. In comparison, animals that received systemic administration of PJ34 starting at 3 h post-TBI demonstrated decreased AIF staining intensity. Higher magnification images indicate the transition of cortical AIF immunofluorescence from punctate cytosolic in sham animals to diffuse (including the nuclear area) distribution in injured animals. PJ34 treatment attenuated these changes. CCI, controlled cortical impact. Color image is available online at www.liebertpub.com/neu

To investigate the effect of delayed PJ34 treatment on spatial learning and memory after TBI, we performed the MWM test from PID 14 to 17. Repeated measures one-way ANOVA did not show a statistically significant interaction between groups and time after injury ($F(6,96) = 0.532$, $p = 0.783$), but the variables groups ($F(2,96) = 6.866$, $p = 0.002$) and time ($F(3,96) = 3.184$, $p = 0.027$) were found to be statistically significant. Student Newman-Keuls *post-hoc* analysis revealed that there was a significant difference between the vehicle-treated TBI group and sham-injured group on PID 17 (Fig. 7B; $p < 0.05$). Similar to the previous study, PJ34 treatment in TBI mice did not improve cognitive function performance in this test as indicated by the mean escape latency on PID 17 that was $61.40 \pm 7.09$ sec for PJ34 TBI and $59.61 \pm 10.12$ sec for vehicle TBI groups.

A probe trial was performed on PID 18. One-way ANOVA followed by Student Newman-Keuls *post-hoc* analysis indicated that both vehicle-treated and PJ34-treated TBI mice spent significantly less time in the target quadrant than sham-injured mice (Fig. 7C; $p < 0.05$ for both). No significant differences were observed between vehicle-treated and PJ34-treated TBI mice. Swim speeds did not differ between the sham-injured, vehicle-treated, and PJ34-treated TBI groups in this test (Fig. 7D).

TBI-induced lesion volumes were quantified in vehicle TBI and PJ34 TBI groups as described previously. TBI resulted in a large lesion in the vehicle-treated group ($7.52 \pm 0.74\ mm^3$), and delayed treatment with PJ34 significantly reduced the TBI-induced lesion volume at 21 DPI ($4.34 \pm 0.72\ mm^3$) (Fig. 8A; $p = 0.003$, Student *t* test). Representative images of vehicle TBI and PJ34 TBI groups are shown.

### *Delayed treatment with PJ34 attenuates neuronal loss in the ipsilateral cortex and thalamus but does not reduce neuronal loss in the ipsilateral hippocampus*

TBI-induced neuronal loss in the cortex, thalamus, CA1, CA2/3, and DG subregions of the hippocampus were quantified on cresyl violet-stained brain sections from sham-injured, vehicle-treated, and delayed PJ34-treated TBI mice at PID 21 using stereological methods. One-way ANOVA and Student Newman-Keuls *post-hoc*

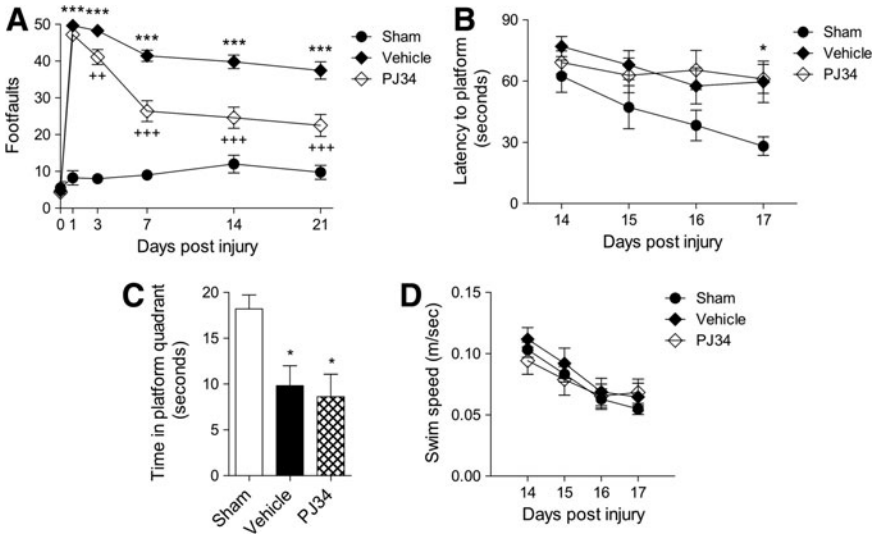


**FIG. 7.** Delayed systemic administration of PJ34 (N-(6-oxo-5,6-dihydro-phenanthridin-2-yl)-N,N-dimethylacetamide) improves sensorimotor function but not cognitive performance after traumatic brain injury (TBI). (**A**) TBI induced significant impairment in motor outcomes at all time points (***$p < 0.001$ vs. sham). There was a statistically significant ''post-injury day X groups'' interaction ($F(8,110) = 6.029$, $p < 0.001$). Systemic administration of PJ34 starting as late as 24 h post-injury significantly improved fine motor coordination at 3 ($^{++}p < 0.01$ vs. vehicle) 7, 14, and 21 days ($^{+++}p < 0.001$ vs. vehicle) post-TBI. Analysis by repeated measures one-way ANOVA, followed by post-hoc adjustments using the Student Newman-Keuls test. Mean ± standard error of the mean (SEM) ($n = 10$ TBI group, $n = 5$ sham-injured group). (**B**) Systemic administration of PJ34 starting at 24 h post-injury did not improve cognitive performance (spatial learning and memory) in the MWM test after TBI. The factors of ''post-injury days'' and ''groups'' were not statistically significant. TBI induced significant cognitive impairments at post-injury days 17 (*$p < 0.05$ vs. sham). PJ34-treated TBI mice demonstrated a latency to locate the submerged platform that was not significantly different compared with vehicle-treated TBI mice. (**C**) In the probe trial, vehicle-treated and/or PJ34-treated TBI mice spent significantly less time in the target quadrant compared with sham-injured mice (*$p < 0.05$). No significant differences were observed between vehicle- and PJ34-treated TBI mice. (**D**) No significant differences in swim speed were observed between sham, vehicle-treated, and PJ34-treated TBI mice. Analysis by repeated measures one-way ANOVA (A, B, D) and one-way ANOVA (C), followed by *post-hoc* adjustments using the Student Newman-Keuls test. Mean ± SEM ($n = 10$ TBI group, $n = 5$ sham-injured group).

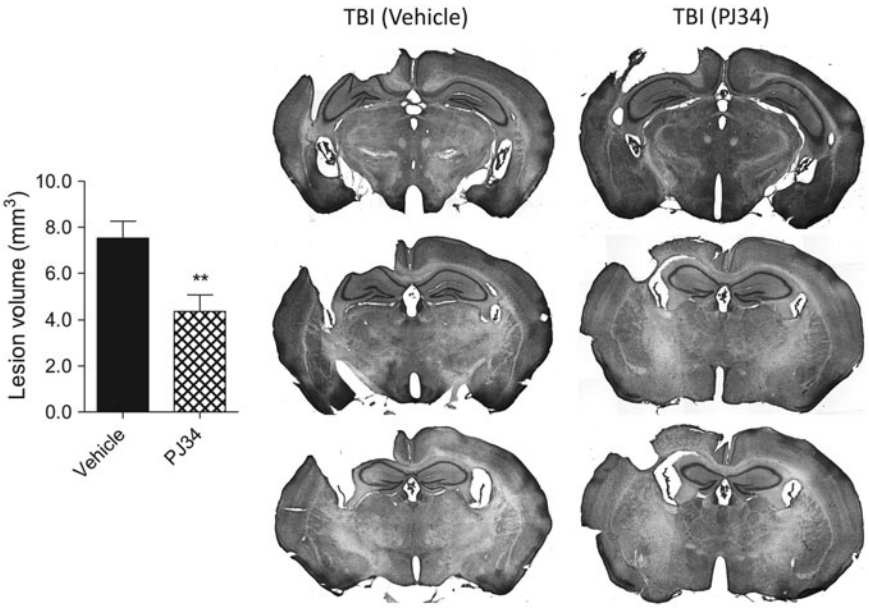


**FIG. 8.** Delayed systemic administration of PJ34 (N-(6-oxo-5,6-dihydro-phenanthridin-2-yl)-N,N-dimethylacetamide) reduces lesion size after traumatic brain injury (TBI). Unbiased stereological assessment of lesion volume at 21 days post-TBI was performed on cresyl violet stained brain sections. PJ34 treatment starting 24 h after TBI significantly reduced the lesion size at 21 days after trauma (**$p < 0.01$ vs. vehicle). Analysis by one-tailed Student *t* test. Mean ± standard error of the mean ($n = 10$/group). Coronal sections across the TBI contusion/lesion from a representative animal in the vehicle-treated and PJ34-treated TBI groups are presented.

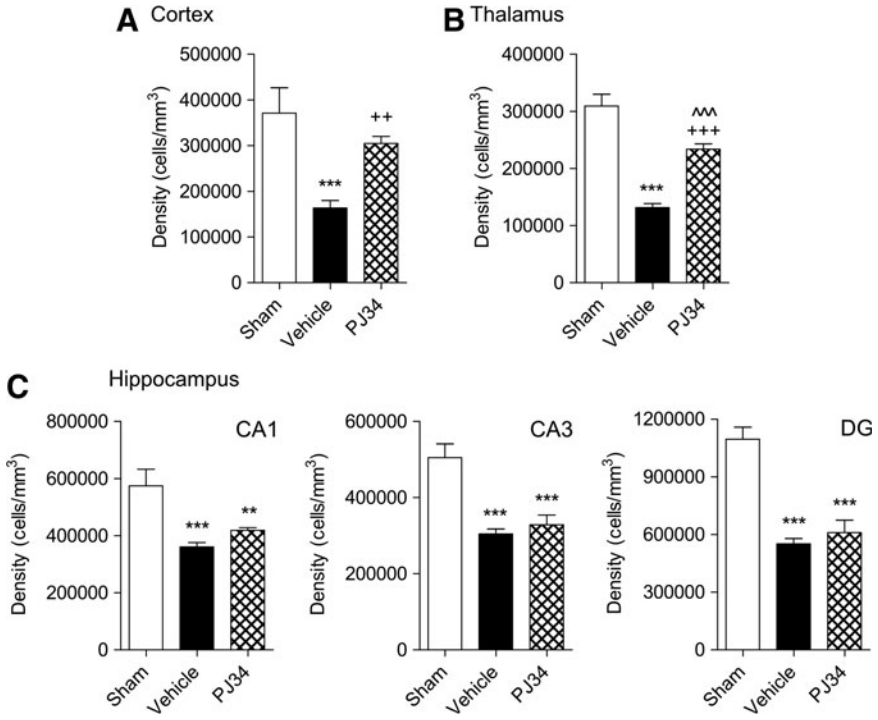


**FIG. 9.** Delayed systemic administration of PJ34 (N-(6-oxo-5,6-dihydro-phenanthridin-2-yl)-N,N-dimethylacetamide) reduces neuronal loss after traumatic brain injury (TBI). Unbiased stereological quantification of neuronal cell loss was performed in the cortex, thalamus as well as the CA1, CA3, and dentate gyrus (DG) subregions of the hippocampus at 21 days post-TBI. TBI caused significant neuronal cell loss in the cortex (**A**), thalamus (**B**), and in the CA1, CA3 and the DG regions (**C**); $***p<0.001$ vs. sham. PJ34 treatment starting 24 h after TBI significantly improved survival of neurons in the cortex (A) and thalamus (B); $^{++}p<0.001$ vs. vehicle, $^{+++}p<0.001$ vs. vehicle, $\text{^^^}p<0.001$ vs. sham. PJ34 treatment starting 24 h after TBI failed to attenuate neuronal loss in the CA1, CA3 and the DG (C) regions of the hippocampus; $**p<0.01$ vs. sham, $***p<0.01$ vs. sham. Analysis by one-way ANOVA, followed by *post-hoc* adjustments using the Student Newman-Keuls test. Mean ± standard error of the mean ($n=5$/group).

analysis demonstrated that TBI resulted in a significant loss of neurons in each region when compared with sham-injured controls (Fig. 9A-C; $p<0.001$ for each). Notably, delayed treatment with PJ34 significantly attenuated the TBI-induced neuronal loss in the cortex (Fig. 9A; $p<0.01$), and there was no significant difference between the sham-injured and PJ34-treated TBI groups. Similarly, PJ34 treatment significantly reduced TBI-induced neuronal loss in the thalamus (Fig. 9B; $p<0.001$), and there was a significant difference in thalamic neuronal densities between the sham-injured and PJ34-treated TBI groups ($p<0.001$). Delayed PJ34 treatment, however, failed to reduce TBI-induced neuronal loss in each subregion of the hippocampus (Fig. 9C; $p>0.05$).

### *Delayed treatment with PJ34 attenuates microglial activation in the injured cortex*

Based on cell morphological features, microglia can be classified into three categories corresponding to increasing activation status:

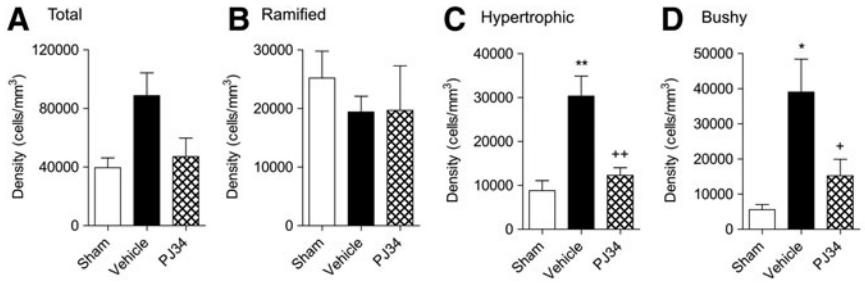


**FIG. 10.** Delayed systemic administration of PJ34 (N-(6-oxo-5,6-dihydro-phenanthridin-2-yl)-N,N-dimethylacetamide) reduces microglia activation aftertraumatic brain injury (TBI). Unbiased stereological quantification of microglial cell densities and activation status in the cortex at 21 days post-injury. Total (**A**), ramified (**B**) representing resting as well as hypertrophic (**C**), and bushy (**D**) representing progressively increased microglial activation phenotypes, respectively, were analyzed. Vehicle-treated animals showed no significant changes in ramified microglia (B) but showed significantly increased numbers of hypertrophic (C; $**p<0.01$ vs. sham) and bushy (D; $*p<0.05$ vs. sham). Systemic administration of PJ34 starting at 24 h after TBI did not significantly change ramified microglia (A) but resulted in significant attenuation in hypertrophic (C; $^{++}p<0.01$ vs. vehicle) and bushy microglia (D; $^{+}p<0.05$ vs. sham). Analysis by one-way ANOVA, followed by *post-hoc* Tukey test. Mean ± standard error of the mean ($n=3$–4/group).

Ramified (resting), hypertrophic, and bushy.[33] Ramified microglia have small cell bodies and thin, long, and highly branched processes. In contrast, hypertrophic microglia have larger cell bodies, with thicker, shorter, and highly branched processes, whereas bushy microglia have multiple short processes that form thick bundles around enlarged cell bodies. TBI results in a transformation of resting ramified microglia within the injured cortex into more highly activated states that display hypertrophic and bushy cell morphological features.[29]

We performed Iba-1 immunohistochemistry to label microglia in the injured cortex and quantified the numbers of microglia in each morphological state at PID 21 using stereological methods. When compared with sham-injured controls, the total numbers of microglia in the injured cortex increased after TBI, and PJ34 treatment reduced the number of microglia (Fig. 10A), but one-way ANOVA followed by Studens Newman-Keuls *post-hoc* analysis failed to demonstrate statistically significant differences between groups.

Further analysis revealed that the numbers of ramified microglia were comparable in the sham-injured, vehicle-treated TBI, and delayed PJ34-treated TBI groups (Fig. 10B). In contrast, there was a significant increase in the number of hypertrophic (Fig. 10C; $p < 0.01$) and bushy (Fig. 10D; $p < 0.05$) microglia in the vehicle-treated TBI group compared with the sham-injured group. Notably, delayed treatment with PJ34 significantly reduced the numbers of both hypertrophic (Fig. 10B; $p < 0.01$) and bushy (Fig. 10C; $p < 0.05$) microglia when compared with the vehicle-treated TBI group. There were no significant differences in numbers of hypertrophic and bushy microglia between the sham-injured and PJ34-treated TBI groups.

## Discussion

Previous studies, using genetic models as well as pharmacological interventions, examined the role of PARP-1 in secondary injury after brain trauma, with mixed results. CCI-induced motor and cognitive deficits were attenuated in PARP-$1^{-/-}$ compared with PARP-$1^{+/+}$ mice, although no reduction in contusion (lesion) volume was observed in the PARP-$1^{-/-}$ mice perhaps because of the decreased brain volume in these animals.[17] Pre-treatment with GPI6150, a PARP-1 inhibitor, in a rat TBI model significantly attenuated the lesion volume but did not reduced the number of TUNEL-positive cells in perilesional cortex when measured 24 h after injury.[34] Systemic administration of a PARP-1 inhibitor (INH2BP) immediately after mouse CCI attenuated PAR increase and NAD + decline, but did not improve motor performance, lesion volume, or hippocampal cell loss.[16] Pre-treatment with PJ34 or INO-1001, an isoindolinone-based PARP-1 inhibitor, via systemic administration in a rat lateral fluid percussion experimental TBI model resulted in a significant attenuation of motor deficits but had no effect on lesion volume.[23] Although moderate doses of INH2BP improved cognitive performance, high doses failed to improve learning deficits after TBI in spite of a stronger PAR attenuation, and the higher dose also adversely impacted performance in sham-injured animals.[16]

Central administration of INO-1001 immediately after mouse CCI attenuated NAD depletion in the brain and modestly improved cognitive function after injury, but did not reduce contusion volume or hippocampal cell loss.[35] INO-1001 also had no negative impact on memory function in sham animals, perhaps because of the lower doses used and/or the absence of global brain exposure.[35]

The cognitive impairments caused by PARP inhibitors may be explained by the ability of PARP to regulate the function of key proteins involved in learning and memory processes via poly-ADP-ribosylation.[16] Indeed, recent data suggest that PARP-1 activity plays a key role in processes such as neurite outgrowth and long-term memory formation.[36,37] PARP-1 is activated in mammalian cortex after treatment with neurotrophins, and increased protein poly-ADP-ribosylation is detected in the cortex and hippocampus after training for memory tasks.[38] Significantly, administration of PJ34 before the ''training'' session impaired long-term memory.[38] Interestingly, uninjured PARP-$1^{-/-}$ mice showed no cognitive deficits and demonstrated significant improvements after TBI when compared with PARP-$1^{+/+}$ mice.[16,17] Further, INH2BP administration had no negative effects in PARP-$1^{-/-}$ mice suggesting that compensatory pathways to control memory functions have developed in these animals, potentially involving other PARP isoforms that are not impacted by PARP-1 inhibitors.[16]

The present work was performed in an effort to clarify the variable functional and histological outcomes of previous experimental TBI studies, and to determine the neuroprotective potential and therapeutic window of the PARP-1 inhibitor, PJ34. We used well-established and sensitive behavioral tests to assess cognitive and motor function recovery in TBI mice treated with PJ34, and we assessed TBI-induced lesion volume, neuronal loss, and microglial activation in these animals using unbiased quantitative stereological analyses.

Administration of PJ34, starting 3 h after CCI, significantly improved motor function performance, attenuated acute neuronal degeneration, and reduced lesion volume at 21 days post-injury. Notably, we also observed a robust improvement in motor function recovery, a significant reduction in lesion volume, and reduced neuronal loss in the cortex and thalamus after TBI when the therapeutic window was extended and PJ34 was administered starting at 24 h post-injury. The fact that PJ34 treatment retains its efficacy even when administered with such an extended therapeutic window greatly increases its clinical potential.

The failure of previous studies to detect therapeutic effects of PJ34 or other PARP-1 inhibitors with regard to lesion volume or neuronal loss after TBI[16,23,35] may in part reflect the lower sensitivity of non-stereological methods, as well as differences in experimental TBI models, and/or drug type/dose. Importantly, we did not observe an improvement in cognitive function performance with PJ34 treatment when administered at 3 or 24 h post-injury, nor did we find a significant neuronal recovery in the CA1, CA3, or DG regions of the hippocampus from PARP-1 inhibition by PJ34 treatment. Whether the inability of PJ34 to improve cognitive performance and neuronal survival in the hippocampus reflects a relative lack of PARP-1 over-activation in this region after TBI, a modest role for PARP1-mediated cell death in the hippocampus, or confounding effects from other hippocampal-specific PARP-1 mechanisms remain unclear and needs further investigation.

The possible negative impact of PARP inhibitors on cognitive outcomes may limit their clinical translation potential, although as discussed above, these observations could reflect dose-dependent effects. Future studies to address these issues should focus on lower PJ34 doses and/or modified administration protocols based on pharmacokinetic data. Further, unlike the present study, these studies should include PJ34-treated non-injured animals to better identify the direct effects of PJ34 on learning and memory.

PARP activation in neurons induced by strong insults such as high N-methyl-D-aspartate concentrations causes ATP depletion leading to impaired function of ATP-dependent ionic pumps and results in cell swelling and necrosis.[22] Studies indicate that PARP-1 inhibition by PJ34, while fully restoring ATP levels, only partially attenuates neuronal cell death, possibly because it may drive the cell death phenotype toward apoptotic mechanisms.[22] ATP levels may be critical in driving the dominant cell death mechanisms, with caspase-dependent apoptosis needing high ATP levels, and necrotic mechanisms predominating under low ATP conditions.[22]

Our data show that MNNG-induced neuronal death is largely PARP-dependent and caspase-independent because PJ34 treatment significantly attenuated MNNG-induced neuronal death, whereas a caspase inhibitor (BOC) had no effect. Intriguingly, PJ34 treatment induces robust caspase activation in neurons exposed to MNNG, suggesting that a switch in cell death mechanisms occurs after PARP inhibition. The overall importance of caspase activation, however, appears relatively modest in the MNNG cell death model because dual PJ34 and caspase inhibitor treatment had no significant additive benefits on neuronal survival.

In certain conditions, PARP-1 activation in neurons may result in a distinct PAR/AIF-mediated type of cell death, parthanatos, which plays a key role in various neuronal injury paradigms such as cerebral hypoxia/ischemia and trauma.[39] Parthanatos induces sequential activation of PARP-1 and generation of PAR polymers leading to their translocation from the nucleus to the mitochondria. PAR-mediated release of AIF from the mitochondria to the nucleus results in DNA degradation and cell death.[30,40] Our studies demonstrate that the release of AIF in the injured brain after TBI is reduced by PJ34 treatment, suggesting that AIF-release is a PARP-dependent process. Attenuation of this cell death mechanism may, in part, account for the neuroprotective effects of PARP-inhibitors after TBI.

Microglial activation plays a key role in secondary injury after TBI by releasing ROS as well as other neurotoxic molecules.[5] PARP-1 stimulates NF-$\kappa$B and/or AP-1 mediated release of matrix metalloproteinase-9 (MMP-9) from activated microglia, which may cause blood–brain barrier (BBB) damage.[41] PJ34 treatment attenuated MMP-9 activation/overexpression after cerebral ischemia, resulting in reduced BBB breakdown and hemorrhagic transformation, as well as reduced infarct volumes and neurological deficits. Increasing doses of PJ34 were associated, however, with a loss of neuroprotection, including higher infarct volume and impaired motor performance after ischemic injury.[41]

PARP-1 may also cause microglial activation after CCI in rats by up-regulating NF-$\kappa$B-dependent transcription of pro-inflammatory genes (e.g., iNOS, ICAM-1, and TNF$\alpha$).[42] A recent study demonstrated that daily treatment with a PARP inhibitor, INO-1001, starting as late as 20 h post-injury and continued for up to 12 days, attenuated post-traumatic microglial activation, reduced neuronal loss, and improved motor function recovery after TBI.[42] PARP inhibition had no effect on TBI-induced lesion volume in this study.[42]

We used two *in vitro* models of microglial activation (LPS and IFN$\gamma$) in BV2 microglia cell line and primary microglia to evaluate the therapeutic effects of PARP-1 inhibition in microglia. PJ34 treatment reduced iNOS expression, as well as release of NO, ROS, TNF$\alpha$, and activation of NF-$\kappa$B in response to LPS stimulation. Our data advance previous observations supporting the hypothesis that the PARP-NF-$\kappa$B pathway is an important component of microglial activation.[43–45] Our *in vivo* studies used quantitative stereological methods coupled with detailed morphological assessment of progressive stages of microglial activation. We demonstrated that systemic administration of PJ34 starting as late as 24 h post-trauma and lasting for 3 days, significantly reduced the number of activated microglia (hypertrophic and bushy morphologies) in the injured cortex at 21 days after TBI. Using the immunohistochemical methods included in the present study we cannot distinguish between proliferation/activation of resident microglia and infiltrating macrophages.

The multipotential activities of PJ34, reflecting its ability to target two independent secondary injury mechanisms, neuronal death and neuroinflammation, may explain its potent therapeutic effects. Interestingly, the ability of PJ34 to inhibit iNOS may also contribute to some of the detrimental effects of PARP inhibition. Previous studies have suggested that iNOS and iNOS-derived NO may attenuate oxidative stress,[46] reduce neuronal loss,[47] and/or stimulate injury-induced neuroregeneration in the hippocampus,[48] activities that promote recovery of memory and learning functions. Future studies should explore PJ34 intervention strategies that minimize the interference of these neuroprotective activities.

A limitation of the present study is the relative lack of selectivity of PJ34. Recent studies showed that PJ34 can also inhibit the serine threonine kinases Pim1 (3.7 mM IC50) and Pim2 (16 mM IC50).[49] Such effects may explain PJ34 modulation of cell cycle activation (CCA), a cell death mechanism in post-mitotic neurons that occurs in a PARP-1 and -2 independent manner.[50] Further, other studies that profiled PJ34 across various members of the PARP family showed that while PJ34 demonstrates high affinity for PARP-1, it also has similar affinity for PARP-2 and only slightly lower affinity for other members of the PARP family and several tankyrase isoforms.[51] Thus, one must be cautious when interpreting the results of studies based exclusively on PJ34 pharmacological interventions.

## Conclusion

Our work highlights the robust neuroprotective potential of PJ34, a PARP-1 inhibitor. PJ34 independently attenuates microglial activation and neuronal cell death *in vitro* and is able after a relatively short, 3-day treatment initiated after a long 24 h therapeutic window to significantly reduce microglial activation, neuronal loss, and motor deficits. Pharmacological interventions targeting PARP activity because of their multipotential neuroprotective properties and extended therapeutic window should be pursued as promising intervention strategies in TBI.

## Acknowledgments

We thank Titilola Akintola, Stephanie Custer, Vladimir Senatorov, and William Jeong for expert technical support. This work was supported by grant RO1 NS061839 to Alan Faden.

## Author Disclosure Statement

No competing financial interests exist.

## References

1. Faul, M., Xu, L., Wald, M.M., Coronado, V.G. (2010). Traumatic brain injury in the United States: emergency department visits, hospitalizations, and deaths. Centers for Disease Control and Prevention, N.C.f.I.P.a.C.: Atlanta.
2. Dutton, R.P., Stansbury, L.G., Leone, S., Kramer, E., Hess, J.R., and Scalea, T.M. (2010). Trauma mortality in mature trauma systems: are we doing better? An analysis of trauma mortality patterns, 1997–2008. J. Trauma 69, 620–626.
3. Stoica, B.A., and Faden, A.I. (2010). Cell death mechanisms and modulation in traumatic brain injury. Neurotherapeutics 7, 3–12.

4. Lau, A., Arundine, M., Sun, H.S., Jones, M., and Tymianski, M. (2006). Inhibition of caspase-mediated apoptosis by peroxynitrite in traumatic brain injury. J. Neurosci. 26, 11540–11553.
5. Loane, D.J. and Faden, A.I. (2010). Neuroprotection for traumatic brain injury: translational challenges and emerging therapeutic strategies. Trends Pharmacol. Sci. 31, 596–604.
6. Phulwani, N.K., and Kielian, T. (2008). Poly (ADP-ribose) polymerases (PARPs) 1–3 regulate astrocyte activation. J. Neurochem. 106, 578–590.
7. Poitras, M.F., Koh, D.W., Yu, S.W., Andrabi, S.A., Mandir, A.S., Poirier, G.G., Dawson, V.L., and Dawson, T.M. (2007). Spatial and functional relationship between poly(ADP-ribose) polymerase-1 and poly(ADP-ribose) glycohydrolase in the brain. Neuroscience 148, 198–211.
8. Shall, S., and de Murcia, G. (2000). Poly(ADP-ribose) polymerase-1: what have we learned from the deficient mouse model? Mutat. Res. 460, 1–15.
9. D'Amours, D., Desnoyers, S., D'Silva, I., and Poirier, G.G. (1999). Poly(ADP-ribosyl)ation reactions in the regulation of nuclear functions. Biochem. J. 342, 249–268.
10. Nguewa, P.A., Fuertes, M.A., Valladares, B., Alonso, C., and Perez, J.M. (2005). Poly(ADP-ribose) polymerases: homology, structural domains and functions. Novel therapeutical applications. Prog. Biophys. Mol. Biol. 88, 143–172.
11. Ju, B.G., Solum, D., Song, E.J., Lee, K.J., Rose, D.W., Glass, C.K., and Rosenfeld, M.G. (2004). Activating the PARP-1 sensor component of the groucho/ TLE1 corepressor complex mediates a CaMKinase IIdelta-dependent neurogenic gene activation pathway. Cell 119, 815–829.
12. Kim, M.Y., Mauro, S., Gévry, N., Lis, J.T., and Kraus, W.L. (2004). NAD+-dependent modulation of chromatin structure and transcription by nucleosome binding properties of PARP-1. Cell 119, 803–814.
13. Kanai, M., Tong, W.M., Sugihara, E., Wang, Z.Q., Fukasawa, K., and Miwa, M. (2003). Involvement of poly(ADP-Ribose) polymerase 1 and poly(ADP-Ribosyl)ation in regulation of centrosome function. Mol. Cell Biol. 23, 2451–2462.
14. Eliasson, M.J., Sampei, K., Mandir, A.S., Hurn, P.D., Traystman, R.J., Bao, J., Pieper, A., Wang, Z.Q., Dawson, T.M., Snyder, S.H., and Dawson, V.L. (1997). Poly(ADP-ribose) polymerase gene disruption renders mice resistant to cerebral ischemia. Nat. Med. 3, 1089–1095.
15. Endres, M., Wang, Z.Q., Namura, S., Waeber, C., and Moskowitz, M.A. (1997). Ischemic brain injury is mediated by the activation of poly(ADP-ribose)polymerase. J. Cereb. Blood Flow Metab. 17, 1143–1151.
16. Satchell, M.A., Zhang, X., Kochanek, P.M., Dixon, C.E., Jenkins, L.W., Melick, J., Szabó, C., and Clark, R.S. (2003). A dual role for poly-ADP-ribosylation in spatial memory acquisition after traumatic brain injury in mice involving NAD+ depletion and ribosylation of 14-3-3gamma. J. Neurochem. 85, 697–708.
17. Whalen, M.J., Clark, R.S., Dixon, C.E., Robichaud, P., Marion, D.W., Vagni, V., Graham, S.H., Virag, L., Hasko, G., Stachlewitz, R., Szabo, C., and Kochanek, P.M. (1999). Reduction of cognitive and motor deficits after traumatic brain injury in mice deficient in poly(ADP-ribose) polymerase. J. Cereb. Blood Flow Metab. 19, 835–842.
18. Iwashita, A., Tojo, N., Matsuura, S., Yamazaki, S., Kamijo, K., Ishida, J., Yamamoto, H., Hattori, K., Matsuoka, N., and Mutoh, S. (2004). A novel and potent poly(ADP-ribose) polymerase-1 inhibitor, FR247304 (5-chloro-2-[3-(4-phenyl-3,6-dihydro-1(2H)-pyridinyl)propyl]-4(3H)-quinazolinone), attenuates neuronal damage in in vitro and in vivo models of cerebral ischemia. J. Pharmacol Exp. Ther. 310, 425–436.
19. Andrabi, S.A., Kim, N.S., Yu, S.W., Wang, H., Koh, D.W., Sasaki, M., Klaus, J.A., Otsuka, T., Zhang, Z., Koehler, R.C., Hurn, P.D., Poirier, G.G., Dawson, V.L., and Dawson, T.M. (2006). Poly(ADP-ribose) (PAR) polymer is a death signal. Proc. Natl. Acad. Sci U S A 103, 18308–18313.
20. Yu, S.W., Andrabi, S.A., Wang, H., Kim, N.S., Poirier, G.G., Dawson, T.M., and Dawson, V.L. (2006). Apoptosis-inducing factor mediates poly(ADP-ribose) (PAR) polymer-induced cell death. Proc. Nat. Acad. Sci. U S A 103, 18314–18319.
21. Lai, Y., Chen, Y., Watkins, S.C., Nathaniel, P.D., Guo, F., Kochanek, P.M., Jenkins, L.W., Szabó, C., and Clark, R.S. (2008). Identification of poly-ADP-ribosylated mitochondrial proteins after traumatic brain injury. J. Neurochem. 104, 1700–1711.
22. Goebel, D.J., and Winkler, B.S. (2006). Blockade of PARP activity attenuates poly(ADP-ribosyl)ation but offers only partial neuroprotection against NMDA-induced cell death in the rat retina. J. Neurochem. 98, 1732–1745.
23. Besson, V.C., Zsengellér, Z., Plotkine, M., Szabó, C., and Marchand-Verrecchia, C. (2005). Beneficial effects of PJ34 and INO-1001, two novel water-soluble poly(ADP-ribose) polymerase inhibitors, on the consequences of traumatic brain injury in rat. Brain Res. 1041, 149–156.
24. Loane, D.J., Stoica, B.A., Pajoohesh-Ganji, A., Byrnes, K.R., and Faden, A.I. (2009). Activation of metabotropic glutamate receptor 5 modulates microglial reactivity and neurotoxicity by inhibiting NADPH oxidase. J. Biol. Chem. 284, 15629–15639.
25. Stoica, B.A., Movsesyan, V.A., Knoblach, S.M., and Faden, A.I. (2005). Ceramide induces neuronal apoptosis through mitogen-activated protein kinases and causes release of multiple mitochondrial proteins. Mol. Cell. Neurosci. 29, 355–371.
26. Loane, D.J., Pocivavsek, A., Moussa, C.E., Thompson, R., Matsuoka, Y., Faden, A.I., Rebeck, G.W., and Burns, M.P. (2009). Amyloid precursor protein secretases as therapeutic targets for traumatic brain injury. Nat. Med. 15, 377–379.
27. Zhao, Z., Loane, D.J., Murray, M.G., 2nd, Stoica, B.A., and Faden, A.I. (2012). Comparing the predictive value of multiple cognitive, affective, and motor tasks after rodent traumatic brain injury. J. Neurotrauma 29, 2475–2489.
28. Kabadi, S.V., Stoica, B.A., Hanscom, M., Loane, D.J., Kharebava, G., Murray Ii, M.G., Cabatbat, R.M., and Faden, A.I. (2012). CR8, a selective and potent CDK inhibitor, provides neuroprotection in experimental traumatic brain injury. Neurotherapeutics 9, 405–421.
29. Byrnes, K.R., Loane, D.J., Stoica, B.A., Zhang, J., and Faden, A.I. (2012). Delayed mGluR5 activation limits neuroinflammation and neurodegeneration after traumatic brain injury. J. Neuroinflammation 9, 43.
30. Yu, S.W., Wang, H., Poitras, M.F., Coombs, C., Bowers, W.J., Federoff, H.J., Poirier, G.G., Dawson, T.M., and Dawson, V.L. (2002). Mediation of poly(ADP-ribose) polymerase-1-dependent cell death by apoptosis-inducing factor. Science 297, 259–263.
31. Slemmer, J.E., Zhu, C., Landshamer, S., Trabold, R., Grohm, J., Ardeshiri, A., Wagner, E., Sweeney, M.I., Blomgren, K., Culmsee, C., Weber, J.T., and Plesnila, N. (2008). Causal role of apoptosis-inducing factor for neuronal cell death following traumatic brain injury. Am. J. Pathol. 173, 1795–1805.
32. Piao, C.S., Loane, D.J., Stoica, B.A., Li, S., Hanscom, M., Cabatbat, R., Blomgren, K., and Faden, A.I. (2012). Combined inhibition of cell death induced by apoptosis inducing factor and caspases provides additive neuroprotection in experimental traumatic brain injury. Neurobiol. Dis. 46, 745–758.
33. Soltys, Z., Ziaja, M., Pawlinski, R., Setkowicz, Z., and Janeczko, K. (2001). Morphology of reactive microglia in the injured cerebral cortex. Fractal analysis and complementary quantitative methods. J. Neurosci. Res. 63, 90–97.
34. LaPlaca, M.C., Zhang, J., Raghupathi, R., Li, J.H., Smith, F., Bareyre, F.M., Snyder, S.H., Graham, D.I., and McIntosh, T.K. (2001). Pharmacologic inhibition of poly(ADP-ribose) polymerase is neuroprotective following traumatic brain injury in rats. J. Neurotrauma 18, 369–376.
35. Clark, R.S., Vagni, V.A., Nathaniel, P.D., Jenkins, L.W., Dixon, C.E., and Szabó, C. (2007). Local administration of the poly(ADP-ribose) polymerase inhibitor INO-1001 prevents NAD+ depletion and improves water maze performance after traumatic brain injury in mice. J. Neurotrauma 24, 1399–1405.
36. Cohen-Armon, M. (2007). PARP-1 activation in the ERK signaling pathway. Trends Pharmacol. Sci. 28, 556–560.
37. Hernandez, A.I., Wolk, J., Hu, J.Y., Liu, J., Kurosu, T., Schwartz, J.H., and Schacher, S. (2009). Poly-(ADP-ribose) polymerase-1 is necessary for long-term facilitation in Aplysia. J. Neurosci. 29, 9553–9562.
38. Goldberg, S., Visochek, L., Giladi, E., Gozes, I., and Cohen-Armon, M. (2009). PolyADP-ribosylation is required for long-term memory formation in mammals. J. Neurochem. 111, 72–79.
39. Wang, Y., Kim, N.S., Li, X., Greer, P.A., Koehler, R.C., Dawson, V.L., and Dawson, T.M. (2009). Calpain activation is not required for AIF translocation in PARP-1-dependent cell death (parthanatos). J. Neurochem. 110, 687–696.
40. Wang, Y., Kim, N.S., Haince, J.F., Kang, H.C., David, K.K., Andrabi, S.A., Poirier, G.G., Dawson, V.L., and Dawson, T.M. (2011). Poly (ADP-ribose) (PAR) binding to apoptosis-inducing factor is critical for PAR polymerase-1-dependent cell death (parthanatos). Sci. Signal. 4, ra20.

41. Haddad, M., Beray-Berthat, V., Coqueran, B., Palmier, B., Szabó, C., Plotkine, M., and Margaill, I. (2008). Reduction of hemorrhagic transformation by PJ34, a poly(ADP-ribose)polymerase inhibitor, after permanent focal cerebral ischemia in mice. Eur. J. Pharmacol. 588, 52–57.
42. d'Avila, J.C., Lam, T.I., Bingham, D., Shi, J., Won, S.J., Kauppinen, T.M., Massa, S., Liu, J., and Swanson, R.A. (2012). Microglial activation induced by brain trauma is suppressed by post-injury treatment with a PARP inhibitor. J. Neuroinflammation 9, 31.
43. Kauppinen, T.M., Higashi, Y., Suh, S.W., Escartin, C., Nagasawa, K., and Swanson, R.A. (2008). Zinc triggers microglial activation. J. Neurosci. 28, 5827–5835.
44. Kauppinen, T.M., Suh, S.W., Higashi, Y., Berman, A.E., Escartin, C., Won, S.J., Wang, C., Cho, S.H., Gan, L., and Swanson, R.A. (2011). Poly(ADP-ribose)polymerase-1 modulates microglial responses to amyloid beta. J. Neuroinflammation 8, 152.
45. Kauppinen, T.M., and Swanson, R.A. (2005). Poly(ADP-ribose) polymerase-1 promotes microglial activation, proliferation, and matrix metalloproteinase-9-mediated neuron death. J. Immunol. 174, 2288–2296.
46. Bayir, H., Kagan, V.E., Borisenko, G.G., Tyurina, Y.Y., Janesko, K.L., Vagni, V.A., Billiar, T.R., Williams, D.L., and Kochanek, P.M. (2005). Enhanced oxidative stress in iNOS-deficient mice after traumatic brain injury: support for a neuroprotective role of iNOS. J. Cereb. Blood Flow Metab. 25, 673–684.
47. Sinz, E.H., Kochanek, P.M., Dixon, C.E., Clark, R.S., Carcillo, J.A., Schiding, J.K., Chen, M., Wisniewski, S.R., Carlos, T.M., Williams, D., DeKosky, S.T., Watkins, S.C., Marion, D.W., and Billiar, T.R. (1999). Inducible nitric oxide synthase is an endogenous neuroprotectant after traumatic brain injury in rats and mice. J. Clin. Invest. 104, 647–656.
48. Zhu, D.Y., Liu, S.H., Sun, H.S., and Lu, Y.M. (2003). Expression of inducible nitric oxide synthase after focal cerebral ischemia stimulates neurogenesis in the adult rodent dentate gyrus. J. Neurosci. 23, 223–229.
49. Antolín, A.A., Jalencas, X., Yélamos, J., and Mestres, J. (2012). Identification of pim kinases as novel targets for PJ34 with confounding effects in PARP biology. ACS Chem. Biol. 7, 1962–1967.
50. Madison, D.L., Stauffer, D., and Lundblad, J.R. (2011). The PARP inhibitor PJ34 causes a PARP1-independent, p21 dependent mitotic arrest. DNA Repair (Amst) 10, 1003–1013.
51. Wahlberg, E., Karlberg, T., Kouznetsova, E., Markova, N., Macchiarulo, A., Thorsell, A.G., Pol, E., Frostell, A., Ekblad, T., Oncu, D., Kull, B., Robertson, G.M., Pellicciari, R., Schuler, H., and Weigelt, J. (2012). Family-wide chemical profiling and structural analysis of PARP and tankyrase inhibitors. Nat. Biotechnol. 30, 283–288.

Address correspondence to:
*Bogdan A. Stoica, MD*
*Department of Anesthesiology*
*University of Maryland, School of Medicine*
*Bressler Research Building*
*655 W. Baltimore Street, Room #6-015*
*Baltimore, MD 21201*

*E-mail:* bstoica@anes.umm.edu